

## Thermodynamic and transport properties of the one-dimensional $S=1/2$ antiferromagnet $\text{Yb}_4\text{As}_3$

Philipp Gegenwart, H. Aoki, T. Cichorek, J. Custers, N. Harrison, M. Jaime, M. Lang, A. Ochiai, F. Steglich

### Angaben zur Veröffentlichung / Publication details:

Gegenwart, Philipp, H. Aoki, T. Cichorek, J. Custers, N. Harrison, M. Jaime, M. Lang, A. Ochiai, and F. Steglich. 2002. "Thermodynamic and transport properties of the one-dimensional  $S=1/2$  antiferromagnet  $\text{Yb}_4\text{As}_3$ ." *Physica B: Condensed Matter* 312-313: 315–20. [https://doi.org/10.1016/s0921-4526\(01\)01526-5](https://doi.org/10.1016/s0921-4526(01)01526-5).

# Thermodynamic and transport properties of the one-dimensional $S = \frac{1}{2}$ antiferromagnet $\text{Yb}_4\text{As}_3$

P. Gegenwart<sup>a,\*</sup>, H. Aoki<sup>a</sup>, T. Cichorek<sup>a</sup>, J. Custers<sup>a</sup>, N. Harrison<sup>b</sup>, M. Jaime<sup>b</sup>,  
M. Lang<sup>c</sup>, A. Ochiai<sup>d</sup>, F. Steglich<sup>a</sup>

<sup>a</sup>Max-Planck Institute for Chemical Physics of Solids, Noethnitzer Str. 48, D-01187 Dresden, Germany

<sup>b</sup>Los Alamos National Laboratory, Los Alamos, New Mexico 87545, USA

<sup>c</sup>Institute for Physics, University of Frankfurt, 60054 Frankfurt (Main), Germany

<sup>d</sup>Center for Low Temperature Science, Tohoku University, Sendai 980-8578, Japan

## Abstract

The semimetallic quasi-one-dimensional  $S = \frac{1}{2}$  antiferromagnet  $\text{Yb}_4\text{As}_3$  has been studied by performing low-temperature ( $T$ ) and high magnetic-field ( $B$ ) measurements of the specific heat,  $C(T, B)$ , magnetization,  $M(T, B)$ , AC-susceptibility,  $\chi_{AC}(T, B)$ , and electrical resistivity,  $\rho(T, B)$ . At finite transverse magnetic fields, a gap  $\Delta(B)$  is induced in the low-energy magnetic excitation spectrum. Our  $C(T, B)$  measurements reveal a  $\Delta(B) \sim B^{2/3}$  dependence for  $B \leq 9$  T, in accordance with predictions of the quantum sine-Gordon model. At higher fields the  $\Delta(B)$  curve levels-off gradually. In the isothermal magnetization taken at 0.6 K no saturation occurs up to 60 T. We also present new results on spin-glass behavior below 0.15 K caused by a weak ferromagnetic interchain coupling and disorder. Finally, we concentrate on the electrical transport properties. Shubnikov-de Haas oscillations, arising from a low-density system of mobile As-4p holes, are recorded in magnetic fields up to 60 T. We estimate the effective mass and the mean-free path of these carriers and discuss spin-splitting effects.

**Keywords:**  $\text{Yb}_4\text{As}_3$ ; One-dimensional Heisenberg chain; Spin glass; Shubnikov-de Haas effect

## 1. Introduction

Quasi-one-dimensional (1D) quantum magnets have been in the focus of intense theoretical and experimental interest for a long time. Antiferromagnetic (AF)  $S = \frac{1}{2}$  Heisenberg chains show gapless two-spinon continuum (or “magnon”) excitations as described by des Cloizeaux and Pearson [1]. A recently studied example is the organic compound Cu-benzoate for which a magnon-derived linear in- $T$  dependence of the low-temperature specific heat has been observed at zero magnetic fields,  $B = 0$  [2].  $B$ -fields that transverse to the  $\text{Cu}^{2+}$  ( $S = \frac{1}{2}$ )-chain direction induce a gap in the low-energy excitations observed by both inelastic-neutron diffraction and

specific-heat experiments [2]. This result is not expected for an AF  $S = \frac{1}{2}$  Heisenberg chain, but was explained within the frame of the quantum sine-Gordon (SG) theory, taking into account a staggered field perpendicular to the chains [3]. While in the insulating Cu-benzoate the spin chains are dictated by the crystal structure at all temperatures, in the rare-earth pnictide compound  $\text{Yb}_4\text{As}_3$  it is a charge-ordering (CO) transition near room temperature [4] which leads to the formation of 1D spin chains at lower  $T$ . At high temperature, in the cubic phase,  $\text{Yb}_4\text{As}_3$  is an intermediate-valence metal with an average valence ratio  $\text{Yb}^{3+}/\text{Yb}^{2+} = 1:3$ . The Yb ions are located on the four interpenetrating families of the cubic space diagonals. At  $T_{CO} \approx 295$  K, driven by intersite Coulomb interactions and a deformation potential coupling to the lattice, the smaller  $\text{Yb}^{3+}$  ions order along one of the cubic space diagonals. The trigonal lattice distortion accompanying

\*Corresponding author. Tel.: +49-351-4646-2324; fax: +49-351-4646-2360.

E-mail address: gegenwart@cpfs.mpg.de (P. Gegenwart).

the CO transition usually results in the formation of a polydomain low- $T$  structure. A preferential orientation of the domains can be induced by the application of a small uniaxial pressure along one space diagonal prior to cooling through  $T_{\text{CO}}$ . The crystal-electric field (CEF) ground state of the  $\text{Yb}^{3+}$  ions can be described by an effective  $S = \frac{1}{2}$  doublet [5]. The  $\text{Yb}^{3+}$  chains are well separated from each other by nonmagnetic  $\text{Yb}^{2+}$  and As ions. The low-energy excitations of these  $S = \frac{1}{2}$  chains have been found using inelastic neutron-scattering (INS) experiments [5] to agree well with the des Cloizeaux–Pearson spectrum of a 1D  $S = \frac{1}{2}$  Heisenberg AF with a nearest-neighbor AF coupling  $|J| = 2.2 \text{ meV}$  (corresponding to  $k_B \cdot 25.5 \text{ K}$ ). Very recently, Shiba et al. [6] showed theoretically that the zero-field ground-state Hamiltonian of the CO variant of  $\text{Yb}_4\text{As}_3$  can be mapped onto the 1D *isotropic*  $S = \frac{1}{2}$  Heisenberg AF. The large heavy-fermion (HF)-like in- $T$  linear contribution to the specific heat,  $\gamma T$ , with  $\gamma = 0.2 \text{ J/K}^2 \text{ mol}$  [7] is in excellent agreement with the expected “magnon” contribution. In the following we consider the CO state of  $\text{Yb}_4\text{As}_3$  as a model system for studying the low-lying excitations of AF  $S = \frac{1}{2}$  chains *despite* the presence of a small number of intrinsic charge carriers.

The paper is organized as follows: After giving details concerning experimental techniques in Section 2, we address in Section 3 the effect of applying transverse magnetic fields to the spin chains. Pulsed-field (60 T) magnetoresistivity and magnetization as well as specific-heat experiments up to 18 T are discussed and compared with recent INS experiments [8] and the theoretical prediction of the quantum sine-Gordon model [9]. In Section 4 we present new results concerning spin-glass behavior at very low temperature caused by weak interchain coupling and disorder. Finally, we address the electrical transport in  $\text{Yb}_4\text{As}_3$  and give a quantitative analysis of Shubnikov-de Haas (SdH) oscillations observed in the isothermal resistivity (Section 5). The conclusions are presented in Section 6.

## 2. Experimental details

The experiments were carried out using high-quality single crystals as described in Ref. [4]. For the specific heat and DC-magnetization measurements, a microcalorimeter from Oxford Instruments and a quantum design SQUID magnetometer were used, respectively. The low- $T$  AC-susceptibility and resistivity were measured by conducting a low-frequency lock-in technique adapted to a  $^3\text{He}/^4\text{He}$  dilution refrigerator. High-field experiments were performed in the Los Alamos High Magnetic Field Laboratory using a short pulse (25 ms) 60 T magnet.

## 3. Field-induced gap

In the following, we discuss the effect of external magnetic fields applied to the AF  $S = \frac{1}{2}$  chains. Upon increasing the field,  $C(T)/T$  becomes progressively reduced below 1 K, while at somewhat higher temperatures a broad hump forms which is shifted with increasing  $B$  continuously towards higher  $T$  [7]. This suggests the opening of a gap in the low-energy excitation spectrum. By a detailed analysis of corresponding anomalies found in the thermal expansion  $\alpha(T, B)$  experiments, where by the application of small uniaxial pressure in domain configuration was varied deliberately, it was shown that a *finite*-field component perpendicular to the short axis (i.e. the  $S = \frac{1}{2}$  chains) is required to induce the anomaly [10]. Several scenarios have been proposed to account for these observations: (i) a very weak interchain coupling [11], (ii) an intrachain dipolar interaction [12], and (iii) solitary excitations described by the *classical* sine-Gordon solution of a 1D Heisenberg AF with a weak easy-plane anisotropy and, in addition, a weak interchain coupling [10]. Within the latter model, the observed minima in the thermal conductivity  $\kappa(B)/\kappa(0)$  are also explained quite naturally assuming a resonant scattering of the three-dimensional phonons by the magnetic solitons [10]. Since the *quantum* sine-Gordon theory can only be applied to the low- $T$  specific heat [9], the *classical* sine-Gordon model as described above had to be used to describe the bumps in  $C(T)/T$  as well as the extrema in the  $T$ -dependencies of both the thermal expansion and the thermal conductivity, which occur at elevated temperatures. This yielded excellent fits to the data for all three

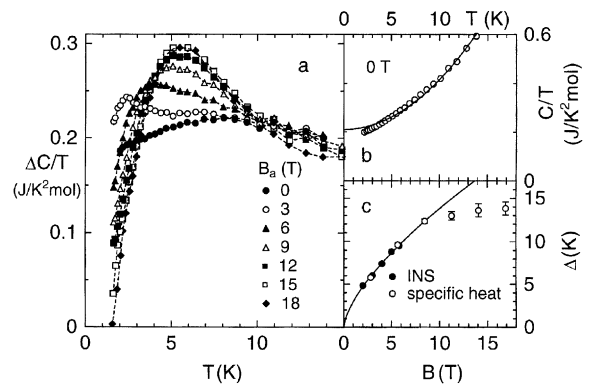


Fig. 1. Specific heat  $C(T)/T$  at varying magnetic fields  $B_a$  applied along the cubic  $\langle 111 \rangle$  direction of polydomain  $\text{Yb}_4\text{As}_3$ . (a)  $\Delta C/T$  denote values after subtraction of phonon contribution  $C_{\text{ph}}/T = \gamma + \beta T^2$  using  $\gamma = 0.21 \text{ J/K}^2 \text{ mol}$  and  $\beta = 2.05 \times 10^{-3} \text{ J/K}^4 \text{ mol}$  indicated by a solid line in (b). (c) Spin-excitation gap  $\Delta$  as derived from inelastic-neutron scattering (INS) [8] and specific heat data (see text).

quantities by allowing for three adjustable parameters in each case [10]. The limitation of the *classical* sine-Gordon model, however, became evident when the field dependence of one of the common fit parameters, the soliton rest energy,  $E_s$ , was determined and observed to obey a power-law dependence:  $E_s \sim B^\nu$ . In contrast to the prediction of the *classical* model,  $\nu = 1$ , however,  $\nu \approx 2/3$  was found to describe the results of the  $C(T, B)$ ,  $\alpha(T, B)$  and  $\kappa(T, B)$  experiments satisfactorily well. Since a  $B^{2/3}$  law is predicted by the *quantum* sine-Gordon theory for the field dependence of the spin gap it was concluded [13] that in a quantum-spin system, the gap and the soliton rest energy have the same origin, while they are independent of each other in the classical model.

The quantum sine-Gordon theory was applied to  $\text{Yb}_4\text{As}_3$  by Oshikawa et al. [9] and Shiba et al. [6]. They showed that the absence of a center of inversion between two adjacent  $\text{Yb}^{3+}$  ions along the chain due to an alternating surrounding of As ions gives rise to a Dzyaloshinskii-Moriya (DM) interaction. The glide reflection with the glide vector parallel to the  $\text{Yb}^{3+}$  chains requires an alternating sign for the DM interaction. An external field with a component perpendicular to the spin-chain direction therefore produces a staggered field. According to Ref. [9] the staggered field induces an excitation gap  $\Delta \sim |J|^{1/3} B^{2/3}$ , where  $B$  is the perpendicular component of the applied field  $B_a$  with respect to the spin chain. Recent INS measurements in  $B \leq 5.8$  T revealed that the spectrum at the 1D wave vector  $\mathbf{q}$  with  $|\mathbf{q}| = \pi/d$  changes drastically from the lower bound of the (two)-spinon continuum found in zero field to a sharp one at finite energy, indicating the opening of an energy gap [8]. The derived  $\Delta(B)$  curve follows the predicted  $B^{2/3}$  dependence (see Fig. 1c).

Here we report on heat-capacity experiments in high magnetic fields which allow us to follow the  $\Delta(B)$  dependence up to higher  $B$ . We have studied a polydomain sample in magnetic fields oriented parallel to one of the four equivalent cubic space diagonals. Therefore, below the CO transition, about 25% of the domains are oriented with the spin chains parallel to the applied field  $B_a$  and about 75% of the domains are aligned such that the effective field component perpendicular to the spin chains is  $B = B_a \sin(70^\circ)$ . Since for the former volume fraction no staggered field is induced, the field dependence observed in Fig. 1 is due to the latter.

$C_{\text{ph}} = \beta T^3$  with  $\beta = 2.05 \times 10^{-3} \text{ J/K}^4 \text{ mol}$  which was obtained from the zero-field measurement (Fig. 1b). The remaining  $\Delta C/T = C(T, B)/T - C_{\text{ph}}/T$  shows maxima corresponding to those observed in thermal expansion [10] whose position shifts to higher  $T$  with increasing fields for  $B_a \leq 12$  T and saturates for higher  $B$ . This result is very different to the prediction of a recent calculation of the specific heat of monodomain  $\text{Yb}_4\text{As}_3$  for elevated  $T$  and transverse magnetic fields up to 24 T

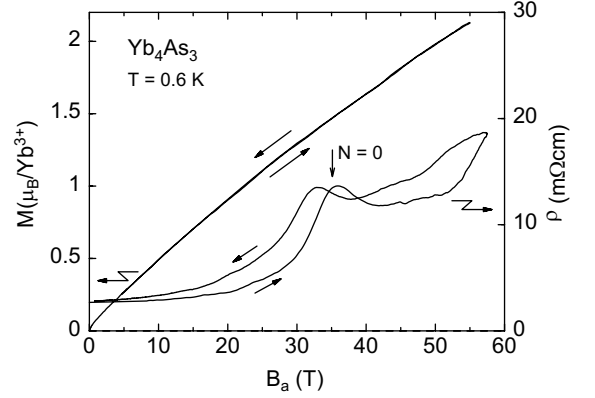


Fig. 2. Pulsed-field DC-magnetization (left axis) and transverse magnetoresistivity (right axis) at 0.6 K for  $B_a$  applied along the cubic  $\langle 111 \rangle$  direction of polydomain  $\text{Yb}_4\text{As}_3$ . Arrows indicate magnetic history and calculated position of the SdH maximum corresponding to the Landau quantum number  $N = 0$  (see text).

using the finite- $T$  density-matrix renormalization-group method by Shibata and Ueda [14]. According to their exact calculation, the result of the quantum sine-Gordon model, that the maxima in  $\Delta C/T$  are located at about  $0.4\Delta$ , is roughly valid up to 24 T which allows us to determine the  $\Delta(B)$  dependence (within 15% error) from our heat-capacity data. As shown in Fig. 1c,  $\Delta(B)$  follows the predicted  $B^{2/3}$  dependence up to 9 T. Upon increasing  $B$  further, the Zeeman energy becomes comparable to the intrachain coupling. This leads to the destruction of the 1D AF state, and a crossover to a ferromagnetic polarization of the spins occurs, accompanied by a flattening of the  $\Delta(B)$  dependence. According to Uimin et al. [12], the excitation gap even disappears at a transverse field  $g_\perp \mu_B B/J \geq 2$  which corresponds, using the  $g$ -value  $g_\perp = 1.2$  determined by polarized-neutron diffraction [15], to  $B \geq 67$  T. To obtain further information on the high-field behavior of  $\text{Yb}_4\text{As}_3$ , we have performed pulsed-field experiments of  $M_{\text{dc}}(B)$  and  $\rho(B)$  at very low temperatures (0.6 K) and up to 60 T applied along the cubic  $\langle 111 \rangle$  direction of our polydomain crystals. As shown in Fig. 2,  $M_{\text{dc}}(B)$  shows a monotonic behavior without any indication for saturation or an additional anomaly. However,  $M_{\text{dc}}(B)$  should be strongly affected by the single-ion CEF excitations. Therefore, besides the contribution of the 1D-spin chains, a large Van Vleck-type contribution is expected which should not saturate up to very high magnetic fields since the highest CEF excitation of the  $J = \frac{7}{2}$  multiplet is located at 29 meV corresponding to a magnetic field of roughly 400 T. The isothermal resistivity  $\rho(B)$  is not affected by the magnetic degrees of freedom of the  $\text{Yb}^{3+}$  chains and the distinct anomalies

are due to the extremely low carrier concentration (see below).

#### 4. Interchain coupling and low- $T$ spin-glass freezing

Using a small uniaxial-pressure cell to induce a monodomain crystal in the CO state, Aoki et al. found an intrinsic upturn in the low- $T$  susceptibility, even for magnetic fields applied parallel to the spin chains [16] which, therefore, cannot be explained by the staggered-field model and must be caused by a weak ferromagnetic interchain coupling [17,18].

To investigate the susceptibility of  $\text{Yb}_4\text{As}_3$  at sufficiently low temperatures, where interchain-coupling effects become important, we measured the ac-susceptibility  $\chi_{ac}$ . The absolute values of  $\chi_{ac}$  have been determined from a comparison in the temperature range  $2\text{ K} \leq T \leq 6\text{ K}$  with the results of the dc-susceptibility measured in 50 mT using the SQUID magnetometer [19]. At  $T = 0.12\text{ K}$ , spin-glass (SG) freezing is observed with the characteristic high sensitivity to small superimposed dc-fields (Fig. 3a). The relative shift  $\delta = \Delta T_f / (\Delta \log(2\pi\nu) T_f)$  of the freezing temperature  $T_f$  per decade in the frequency of the ac-field,  $\nu$ , is estimated as  $\delta = 0.03 \pm 0.005$ , i.e. a value between that found for metallic and insulating spin-glasses (Fig. 3b) [20]. A uniaxial-pressure experiment of the low- $T$  ac-susceptibility showed that the SG freezing is not affected by domain disorder [21]. The *antiferromagnetic* intrachain coupling together with the weak *ferromagnetic* interchain coupling leads to frustration along the chains. Taken together with the disorder that is present on the  $\text{Yb}^{3+}$ -chains inferred, e.g. from the relative short carrier mean-free path obtained from SdH experiments as described below, the SG-freezing effects can be understood quite naturally.

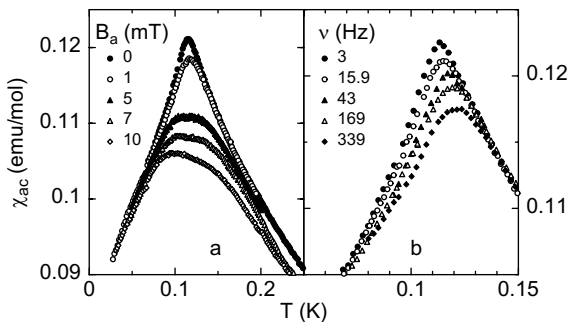


Fig. 3. Temperature dependence of the ac-susceptibility ( $B_{ac} = 0.1\text{ mT}$ ) in different fields  $B_a$  applied along the cubic  $\langle 111 \rangle$  direction of polydomain  $\text{Yb}_4\text{As}_3$  (a) and taken at different frequencies  $\nu$  (b) in  $B_a = 0$ .

#### 5. Resistivity and Shubnikov-de Haas effect

In the CO state,  $\text{Yb}_4\text{As}_3$  is a compensated semimetal, with 3D charge carriers: the number of light and mobile As-4p holes exactly equals the number of heavy Yb-4f electrons in the partially filled 4f hole level [23]. Most remarkably, the electrical resistivity  $\rho(T)$  shows typical HF-like behavior [4], i.e. a  $\rho(T) - \rho_0 = aT^2$  dependence between 4 and 20 K with a huge coefficient  $a$  (Fig. 4a). However, due to the low-carrier concentration of the order of  $10^{-3}/\text{f.u.}$  [4], the usual Kondo-scenario underlying HF physics can be excluded. Interestingly enough, the large coefficient  $a$  remains almost unchanged up to 18 T [19], while the specific-heat coefficient  $\gamma$  rapidly decreases due to the gap formation [7]. This strongly suggests that it is the scattering of the light and mobile As-4p holes by the heavy Yb-4f electrons as opposed to scattering by the magnon-like excitations (cf. Ref. [23]) that leads to the large coefficient  $a$  in resistivity. At lower temperatures,  $\rho(T)$  deviates from the  $T^2$  behavior, passes through a minimum at 2 K followed by a 0.15% increase and saturation below 0.1 K (Fig. 4b). The increase of the low- $T$  resistivity is very probably related to the SG effects. The isothermal resistivity (Fig. 4c) roughly follows a  $B^2$  behavior with superimposed SdH oscillations as has also been observed by Aoki et al. [22]. According to LSDA + U band-structure calculations, both the hole and electron sheets of the Fermi surface are almost spherical [23]. We expect the SdH oscillations to arise from the light As-4p holes since their mobility is much larger than that of the much heavier Yb-4f electrons. In the magnetic-field interval  $B = 4.5\text{--}12\text{ T}$ , an SdH frequency  $f = 25\text{ T}$  is found similar as reported in [22]. The oscillations result from

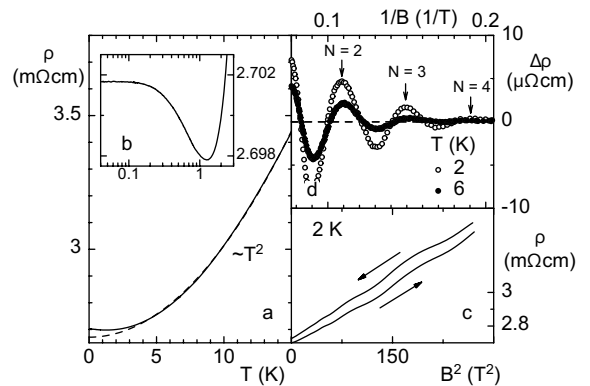


Fig. 4. Electrical resistivity for polydomain  $\text{Yb}_4\text{As}_3$ , plotted as  $\rho$  vs.  $T$  (a),  $\rho$  vs.  $\log(T/K)$  (b), and  $\rho$  vs.  $B^2$  (c). The dashed line in (a) represents  $\Delta\rho(T) = 3.4\text{ }\mu\Omega\text{cm/K}^2 T^2$ , the arrows in (c) indicate magnetic history of the data. The vertical shift in (c) is due to relaxation. (d): SdH oscillations at two different temperatures. Arrows indicate Landau quantum numbers  $N$  of the observed maxima in the SdH effect.

the depopulation of the Landau tubes  $N = 4, 3$  and  $2$  (Fig. 4d). Assuming one pair of As-4p bands as derived from LSDA+U band-structure calculations [23], the observed frequency of 25 T would correspond to a carrier concentration  $n \approx 1.4 \times 10^{18} \text{ cm}^{-3}$ , whereas the low- $T$  Hall coefficient  $R_H$  determined on the same single crystal reveals a two times larger value of  $(eR_H)^{-1} \approx 3 \times 10^{18} \text{ cm}^{-3}$  [18]. The reason for this discrepancy is unclear yet and needs further theoretical investigations.

For  $B \geq 12.5 \text{ T}$  additional oscillations are observed, which might be related to spin splitting because of the extremely low-carrier concentration, the system is already in the quantum limit. Assuming a splitting  $v_s = 0.016 \text{ T}^{-1}$  of the  $N = 1$  maximum (see dotted lines in Fig. 5), the effective Landé  $g$ -factor for the As-4p holes given by  $g_{\text{eff}} = 2v_s f / (m_{\text{eff}}^* / m_0)$  is calculated as  $2.9 \pm 0.2$ . Here we used the effective carrier mass  $m_{\text{eff}}^* = (0.275 \pm 0.005)m_0$  determined from the analysis of the  $T$ -dependence of the SdH oscillations in low fields (Fig. 6a). It is difficult to analyze the several additional oscillations in the SdH effect found for  $B \geq 20 \text{ T}$  (Fig. 5), except for a pronounced peak in  $\rho(B)$  developing around 35 T: at this field, the SdH maximum related to  $N = 0$  should appear (see Fig. 2).

The analysis of the field dependence of the oscillations below 8.5 T taken at differing temperatures, reveals a Dingle temperature of  $T_D = 6.6 \text{ K}$  corresponding to a charge-carrier mean-free path of  $\approx 215 \text{ \AA}$ . We note that the magnon mean-free path along the  $S = \frac{1}{2}$  chains determined from the  $B = 0$  thermal conductivity is roughly  $500 \text{ \AA}$  [18], and that both values are much smaller than the domain size of approximately  $1 \mu\text{m}$ .

Finally, we address the pronounced hysteresis of the electrical resistivity upon increasing and decreasing  $B$

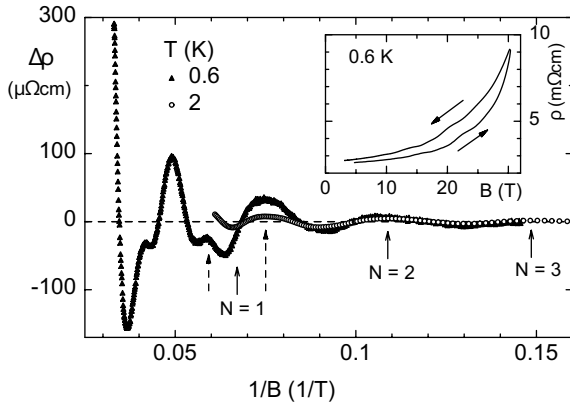


Fig. 5. SdH oscillations for  $\text{Yb}_4\text{As}_3$ , obtained at 2 K from the data shown in Fig. 4c and at 0.6 K from pulsed-field data shown in the inset. Landau quantum numbers  $N$  are indicated by arrows. Spin splitting of  $N = 1$  orbit is indicated by dotted lines.

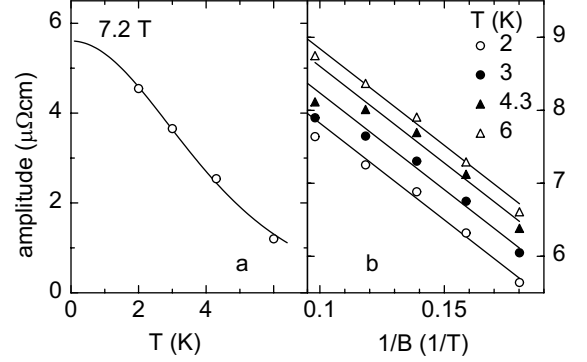


Fig. 6. (a)  $T$ -dependence of the SdH oscillations at 7.2 T (symbols) and a fit to the standard Lifshitz and Kosevich theory (solid line). (b) Dingle-plot of  $\log(\text{amplitude} \cdot B^{1/2} \sinh(14.69 T/K m^*/m_0 T/B))$  vs.  $1/B$ . From the slope of the solid lines a Dingle temperature of  $T_D = 6.6 \text{ K}$  is estimated.

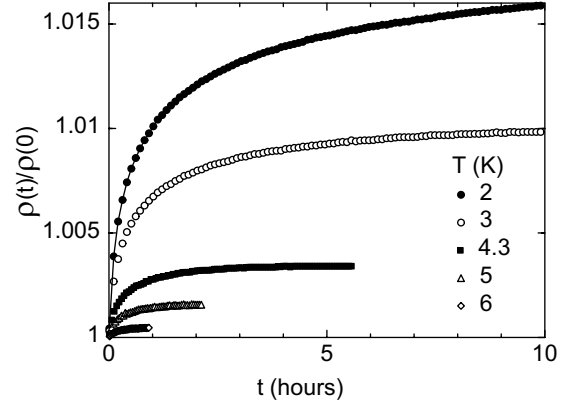


Fig. 7. Relaxation of the electrical resistivity in  $B = 16.5 \text{ T}$  (applied with a rate of  $0.25 \text{ T/min}$ ), plotted as  $\rho(t)/\rho(0)$  vs. time,  $t$ , at different temperatures.

(Figs. 2 and 4c and Inset Fig. 5) as well as upon warming and cooling in  $B > 0$  [19]. To further study this effect which was also observed on a monodomain single crystal [19], we recorded the time-dependence of the resistivity  $\rho(t)$  after the application of 16.5 T over 10 h at several temperatures below 7 K (Fig. 7). A pronounced relaxation was found which does not saturate after 10 h and cannot be fitted to a simple logarithmic decay. This relaxation effect increases with decreasing  $T$ , reaching about 1.5% at 2 K. The origin of the hysteresis loop and relaxation in the resistivity has been unclear until now. It might be related to a slow motion of static point defects: No corresponding hysteresis was found in the dc-magnetization  $M(B)$  (Fig. 2) and no relaxation larger than 0.1% at 2 K was observed in  $M(t)$ , measured by using a SQUID magnetometer after the application of 7 T [24].

## 6. Conclusion

We have presented new thermodynamic and transport experiments on the low-carrier density  $S = \frac{1}{2}$  antiferromagnet  $\text{Yb}_4\text{As}_3$ . Finite transverse magnetic fields (i) open a gap  $\Delta(B)$  in the low-energy excitations and (ii) lead to soliton-like anomalies in thermodynamic properties and the phonon thermal conductivity. These two types of phenomena are not independent of, but are closely related to each other. The magnetic-field dependence of  $\Delta(B)$  was found to follow the  $B^{2/3}$  dependence predicted by the quantum-sine-Gordon model for  $B \leq 9$  T. At higher fields,  $\Delta(B)$  levels-off gradually. In the dc-magnetization no indication for a phase transition is observed up to 60 T. Disorder, together with a weak ferromagnetic coupling between the AF chains, leads to a low- $T$  SG transition at 0.12 K. The transport properties, arising from the 3D semimetallic character of  $\text{Yb}_4\text{As}_3$ , were investigated down to very low temperatures ( $T \geq 20$  mK) and up to very high magnetic fields ( $B \leq 60$  T). A detailed analysis of the SdH oscillations confirms the existence of a small concentration of light As-4p holes. The HF-like resistivity observed even in high magnetic fields where the large  $B = 0$  in- $T$  linear specific heat is suppressed, suggests a two-band model of current-carrying As-derived 4p-holes scattered by heavy Yb-derived 4f electrons.

## Acknowledgements

We gratefully acknowledge stimulating discussions with M. Kohgi, K. Iwasa, T. Suzuki, B. Schmidt, P. Thalmeier, A. Yaresko, N. Shibata and K. Ueda.

## References

- [1] J. des Cloizeaux, J.J. Pearson, Phys. Rev. 128 (1962) 2131.
- [2] D.C. Dender, P.R. Hammar, D.N. Reich, C. Broholm, G. Aeppli, Phys. Rev. Lett. 79 (1997) 1750.
- [3] M. Oshikawa, I. Affleck, Phys. Rev. Lett. 79 (1997) 2883.
- [4] A. Ochiai, T. Suzuki, T. Kasuya, J. Phys. Soc. Japan 59 (1990) 4129.
- [5] M. Kohgi, K. Iwasa, J.-M. Mignot, A. Ochiai, T. Suzuki, Phys. Rev. B 56 (1997) R11388.
- [6] H. Shiba, K. Ueda, O. Sakai, J. Phys. Soc. Japan 69 (2000) 1493.
- [7] R. Helfrich, M. Köppen, M. Lang, F. Steglich, A. Ochiai, J. Magn. Magn. Mater. 177–181 (1998) 309.
- [8] M. Kohgi, K. Iwasa, J.-M. Mignot, B. Fåk, P. Gegenwart, M. Lang, A. Ochiai, H. Aoki, T. Suzuki, Phys. Rev. Lett. 86 (2001) 2439.
- [9] M. Oshikawa, K. Ueda, H. Aoki, A. Ochiai, M. Kohgi, J. Phys. Soc. Japan 68 (1999) 3181.
- [10] M. Köppen, M. Lang, R. Helfrich, F. Steglich, P. Thalmeier, B. Schmidt, B. Wand, D. Pankert, H. Benner, H. Aoki, A. Ochiai, Phys. Rev. Lett. 82 (1999) 4548.
- [11] B. Schmidt, P. Thalmeier, P. Fulde, Europhys. Lett. 35 (1996) 109.
- [12] G. Uimin, Y. Kudasov, P. Fulde, A. Ovchinnikov, Eur. Phys. J. B 16 (2000) 241.
- [13] F. Steglich, M. Köppen, P. Gegenwart, T. Cichorek, B. Wand, M. Lang, P. Thalmeier, B. Schmidt, H. Aoki, A. Ochiai, Acta Phys. Pol. 97 (2000) 91.
- [14] N. Shibata, K. Ueda, J. Phys. Soc. Jpn. 70 (2001) 3690.
- [15] K. Iwasa, M. Kohgi, A. Gukasov, J.-M. Mignot, N. Shibata, A. Ochiai, H. Aoki, T. Suzuki, J. Magn. Magn. Mater. 226–230 (2001) 441.
- [16] H. Aoki, A. Ochiai, M. Oshikawa, K. Ueda, Physica B 281&282 (2000) 465.
- [17] H. Aoki, Ph.D. Thesis, Tohoku University, 2000, unpublished.
- [18] B. Schmidt, H. Aoki, T. Cichorek, J. Custers, P. Gegenwart, M. Kohgi, M. Lang, C. Langhammer, A. Ochiai, S. Paschen, F. Steglich, T. Suzuki, P. Thalmeier, B. Wand, A. Yaresko, Phys. B 300 (2001) 121.
- [19] P. Gegenwart, T. Cichorek, J. Custers, M. Lang, H. Aoki, A. Ochiai, F. Steglich, J. Magn. Magn. Mater. 226–230 (2001) 630.
- [20] J. Mydosh, Spin Glasses: an Experimental Introduction, Taylor & Francis, London, Washington DC, 1993.
- [21] P. Gegenwart, et al., to be published.
- [22] H. Aoki, A. Ochiai, N. Kimura, T. Terashima, C. Terakura, H. Harima, J. Phys. Soc. Jpn., submitted.
- [23] V.N. Antonov, A.N. Yaresko, A.Ya. Perlov, P. Thalmeier, P. Fulde, P.M. Oppeneer, H. Eschrig, Phys. Rev. B 58 (1998) 975.
- [24] P. Gegenwart, H. Aoki, T. Cichorek, J. Custers, M. Jaime, A. Ochiai, F. Steglich, Pramana-J. Phys., submitted.